

The Ultraviolet Spectral Energy Distributions of Quiescent Black Holes and Neutron Stars

R.I. Hynes

Department of Physics and Astronomy, Louisiana State University, Baton Rouge, Louisiana 70803
 rih@phys.lsu.edu

E. L. Robinson

Department of Astronomy, The University of Texas at Austin, 1 University Station C1400, Austin, Texas 78712
 elr@astro.as.utexas.edu

ABSTRACT

We present *HST*/ACS ultraviolet photometry of three quiescent black hole X-ray transients: X-ray Nova Muscae 1991 (GU Mus), GRO J0422+32 (V518 Per), and X-ray Nova Vel 1993 (MM Vel), and one neutron star system, Aql X-1. These are the first quiescent UV detections of these objects. All are detected at a much higher level than expected from their companion stars alone and are significant detections of the accretion flow. Three of the four UV excesses can be characterized by a black body of temperature 5000 – 13,000 K, hotter than expected for the quiescent outer disk. A good fit could not be found for MM Vel. The source of the black-body-like emission is most likely a heated region of the inner disk. Contrary to initial indications from spectroscopy there does not appear to be a systematic difference in the UV luminosity or spectral shape between black holes and neutron star systems. However combining our new data with earlier spectroscopy and published X-ray luminosities there is a significant difference in the X-ray to UV flux ratios with the neutron stars exhibiting L_X/L_{UV} about $10\times$ higher than the black hole systems. This is consistent with earlier comparisons based on estimating non-stellar optical light, but since both bandpasses we use are expected to be dominated by accretion light we present a cleaner comparison. This suggests that the difference in X-ray luminosities cannot simply reflect differences in quiescent accretion rates and so the UV/X-ray ratio is a more robust discriminator between the black hole and neutron star populations than the comparison of X-ray luminosities alone.

Subject headings: accretion, accretion discs—binaries: close—stars: individual: GU Mus—stars: individual: V518 Per—stars: individual: MM Vel—stars: individual: Aql X-1

1. Introduction

The discovery that many transient X-ray sources contain stellar mass black holes has provided many opportunities to study the astrophysics of how black holes accrete matter. These black hole X-ray transients (BHXRTs) and their neutron star counterparts (NSXRTs) are low-mass X-ray binaries (LMXBs) in which a companion

star, typically a dwarf or sub-giant of solar mass or less accretes onto the compact object through an accretion disk. The combination of large dynamic range of behavior observed in these objects, and accessible timescales on which to study their variations through this range are unique to the stellar mass objects but may also illuminate the snapshots of a particular state seen in supermassive black holes.

One of the most interesting aspects of this study is to observe quiescent LMXBs in which the outer parts of the accretion disk are cool and dim and the mass transfer onto the compact object proceeds at an extremely low rate; in XTE J1118+480 McClintock et al. (2003) inferred an accretion rate of only $10^{-8.5}$ of the Eddington limit. Accretion in this regime is expected to proceed very differently as the inner disc is unstable to evaporation into a vertically extended, radiatively inefficient accretion flow. Because of the radiative inefficiency, it is possible for gas heated by viscosity to either deposit the heat on the neutron star surface or carry it through a black hole event horizon before it can radiate away. In the neutron star case the energy will eventually escape whereas in the black hole case it will not, leading to the naive expectation, apparently supported by observations, that quiescent neutron stars should be systematically brighter than black holes (Narayan, Garcia, & McClintock 1997; Garcia et al. 2001; Hameury et al. 2003). The observational claim has led to great controversy, however, and objections have been raised to this simple picture. For example, it is necessary to compare objects which are believed to be accreting at the same rate from their companion stars. Menou et al. (1999) argued that this was the case if Eddington-scaled X-ray luminosities of black holes and neutron stars of the same orbital period were compared. Questions were also raised about whether significant amounts of accretion energy may be carried by the bulk motion of a jet (Fender, Gallo, & Jonker 2003). Finally, there is one NSXRT, 1H 1905+000, which appears to defy the trend (Jonker et al. 2007) being fainter than comparable black hole systems. Observations beyond just a comparison of X-ray luminosities are needed.

One promising avenue to improve on this situation is the ultraviolet. Unlike the optical emission which appears dominated by the companion star, UV observations with *HST*/FOS of a quiescent black hole revealed a significant blue excess attributed to accretion light (McClintock et al. 1995). Subsequent more sensitive spectroscopic observations have been performed with STIS of two black holes, A 0620–00 (McClintock & Remillard 2000) and XTE J1118+480 (McClintock et al. 2003) and one neutron star,

Cen X-4 (McClintock & Remillard 2000) and have confirmed this excess, as have more recent COS observations of A 0620–00 (Froning et al. 2011). Intriguingly in the two black hole systems the flux dropped off steeply in the UV, whereas in Cen X-4 it actually rose (in νF_ν) leading to the suggestion that the shape of the UV spectrum is a diagnostic of the presence of a black hole or neutron star.

Clearly such a conclusion based on a sample of three UV spectra is unsatisfactory; but spectroscopic observations of other (fainter) objects become prohibitively expensive, even with the Cosmic Origins Spectrograph. To expand the sample, we present here UV photometry performed with *HST*/ACS of three more black holes, X-ray Nova Mus 1991 = GU Mus, GRO J0422+32 = V518 Per, and X-ray Nova Vel 1993 = MM Vel, and one more neutron star, Aql X-1. Together with the three spectroscopic observations discussed earlier, and the UV photometry of V404 Cyg reported separately by Hynes et al. (2009) this more than doubles the sample available for comparison.

2. Observations

Ultraviolet photometry used the Advanced Camera for Surveys (ACS; Gonzaga et al. 2005) on the *Hubble Space Telescope* (*HST*). The observations are summarized in Table 1. For each target 2 or 3 satellite orbits were used, with all filters observed in each orbit in the sequence F330W–F250W–F220W–F330W. This provides some averaging over variability and ensures each short wavelength observation is bracketed by nearby F330W ones.

Reduction used standard ACS techniques. Individual images were pre-processed to the flat-fielded stage using the automatic pipeline, CALACS; we found no need to refine this reduction. All of the images, or an orbit-by-orbit subset, were then combined offline into a geometrically corrected master image using Multidrizzle (Koekemoer et al. 2002) with standard settings. We found excellent registration between individual images.

Photometry was performed using the IDL/AstroLib aperture photometry routine APER. As our targets are faint we used a relatively small aperture to perform photometry, of radius $0.125''$, with sky

defined by a $2.5''$ annulus. Other stars in the field were typically too faint to determine per-field aperture corrections, so we use the tabulated values from Sirianni et al. (2005). The aperture collects about 75% of the total light, and almost all of the sharp core of the point spread function. In each case, the position of the target was measured in the F330W bandpass and then fixed for the other filters, after verifying that brighter stars were consistently positioned in all the filters.

A significant source of systematic uncertainty in ACS photometry is charge transfer inefficiency (CTI) due to radiation damage to the CCDs (Riess & Mack 2004; Pavlovsky et al. 2005). This is worst at low light levels, so maximized for faint sources in the UV. CTI is also least well calibrated for these cases, and the correction prescriptions provided by Pavlovsky et al. (2005) formally diverge for negligible sky background or source counts. For the low background case ($0.5\text{--}1.5e^-/\text{pixel}$) at source brightnesses up to a few hundred electrons, Riess & Mack (2004) found losses of around 0.035 mag at maximum distance from the readout amplifier from actual data. If we rescale this to the times of our observations and positions of the sources we find losses of 4–7%. We use these latter estimates to correct our measured source brightnesses (or upper limits) and assign an additional error estimate of 2% for most cases to account for the uncertainty in applying CTI corrections. We increase this error estimate to 3% for V518 Per as this was the last observation made, hence subject to the largest detector degradation, and was the faintest source. In F220W observations that did not detect a source, the brightness is beyond the regime calibrated by Riess & Mack (2004) and we increase the CTI correction error estimate to 5%. The uncertainties in the CTI corrections are always much smaller than the statistical uncertainties in the measured fluxes and so do not significantly affect our conclusions.

We tabulate our photometric results in Table 1. Since we are measuring counts across a broad bandpass rather than monochromatic fluxes, we tabulate the data in two ways: the corrected number of electrons per second and the average flux per unit wavelength. Both have been corrected for CTI, and to a nominally infinite aperture.

3. Astrometry

Several of our targets are known to have nearby contaminating stars in the optical or IR which have been barely resolved. *HST* images provide an ideal opportunity to obtain more precise relative astrometry of the contaminating stars if they can be identified. We detected the stars near MM Vel (Filippenko et al. 1999) and Aql X-1 (Chevalier et al. 1999). We were unable to detect the star north-east of V518 Per reported by Reynolds, Callanan, & Filippenko (2007).

The F330W image of MM Vel is shown in Fig. 1. Star identifications are taken from Filippenko et al. (1999). The close blend of stars seen by Filippenko et al. (1999) is well resolved and no new stars are detected. The separation of MM Vel from star A is $\Delta\alpha = -0.048''$, $\Delta\delta = +1.37''$, corresponding to a separation $1.47''$, roughly consistent with the estimate of Filippenko et al. (1999) that MM Vel was 1.6 arcsec north-north-west of star A.

We show the F330W image of Aql X-1 in Fig. 1. Star identifications are taken from Chevalier et al. (1999). Aql X-1 is star (e), much brighter relative to star (a) than it is in the *I* band. Star (b) is weakly detected, but stars (c) and (d) are undetected in this bandpass. We find no new stars in the immediate vicinity of Aql X-1. The separation of Aql X-1 from star (a) is $\Delta\alpha = -0.031''$, $\Delta\delta = +0.07''$, corresponding to a separation $0.48''$, consistent with that found by Chevalier et al. (1999).

4. Adopted Parameters and Archival Measurements

4.1. GU Mus = X-ray Nova Muscae 1991

For the reddening and distance to GU Mus, we follow Hynes (2005) and do not repeat the arguments made there; see that work for the original references. These were a reddening of $E(B - V) = 0.30 \pm 0.06$ and distance $d = 5.89 \pm 0.26$ kpc. The spectral type of GU Mus has been estimated as K3–K5V (Orosz et al. 1996) and K3–K4V (Casares et al. 1997). A K4V classification implies an effective temperature around 4550 K interpolating on the tables in Cox (2000). Using the system parameters from Gelino, Harrison, & McNamara (2001), including a 10.38 hr orbital period, we expect a surface gravity of $\log g = 4.32$.

Quiescent photometry was compiled by Gelino, Harrison, & McNamara (2001) from both their own observations and those of Remillard, McClintock, & Bailyn (1992), Orosz et al. (1996), King, Harrison, & McNamara (1996), and della Valle, Masetti, & Bianchini (1998). These results are quite varied, with V magnitudes ranging from 20.35 to 20.83. This variability is consistent with the large amplitude quiescent variations seen by Hynes et al. (2003) and indicates that non-simultaneous optical photometry cannot reliably be combined with our UV data.

4.2. V518 Per = GRO J0422+32

As for GU Mus, we follow Hynes (2005) and adopt $E(B - V) = 0.35 \pm 0.10$ and $d = 2.49 \pm 0.30$ kpc. Opinion on the spectral type of V518 Per is divided. Early estimates favored early M spectral types: M0–M4V (Casares et al. 1995) or M1–M4V (Harlaftis et al. 1999). Webb et al. (2000) favored slightly later types, M4–M5V, but Gelino & Harrison (2003) argued that the spectral energy distribution was best fit by an M1V star. Gelino & Harrison (2003) assumed negligible disk contamination even in the optical, however, whereas the other authors cited found significant amounts (above 50%), suggesting that a later spectral type with blue contamination may indeed be a better description. In fact, Reynolds, Callanan, & Filippenko (2007) find substantial flickering even in the near-IR, so a spectral type determined from the SED should be viewed with considerable caution. We therefore consider both M1V and M5V classifications, adopting effective temperatures of 3680 K and 3170 K respectively. Using the system parameters of Gelino & Harrison (2003), including a 5.09 hr orbital period, implies a surface gravity of $\log g = 4.66$.

For optical/IR photometry we use data from Zhao et al. (1994), Casares et al. (1995), Garcia et al. (1996), Callanan et al. (1996), Chevalier & Ilovaisky (1996), Gelino & Harrison (2003), and Reynolds, Callanan, & Filippenko (2007). As for GU Mus, substantial variations occur from epoch to epoch.

4.3. MM Vel = X-ray Nova Velorum 1993

For MM Vel, we follow Hynes (2005) and adopt $E(B - V) = 0.20 \pm 0.05$ and $d = 3.82 \pm 0.27$ kpc. The most persuasive spectral type determination

is that by Filippenko et al. (1999) who find a spectral type of K7–M0V, although not rejecting K6V strongly. Other authors preferred earlier spectral types (Shahbaz et al. 1996; della Valle et al. 1997). We will adopt K7V as a compromise, implying an effective temperature of 4180 K. Using the system parameters of Gelino (2004) together with the 6.86 hr orbital period of Shahbaz et al. (1996) implies a surface gravity of $\log g = 4.55$.

Published quiescent photometry of this object is much sparser than for GU Mus and V518 Per, limited to R band measurements of Shahbaz et al. (1996) and Filippenko et al. (1999), and V band by Hynes et al. (2003).

4.4. Aql X-1

The interstellar reddening to Aql X-1 has been estimated at $E(B - V) = 0.5 \pm 0.1$. Although Chevalier et al. (1999) estimate a distance of $d = 2.5$ kpc, Rutledge et al. (2001) argue that this is too low and instead obtain a distance of 4.0–6.5 kpc by requiring that the companion must fill its Roche lobe, and using the peak luminosity of photospheric radius expansion X-ray bursts. They adopt a preferred distance of 5 kpc and we follow this. The companion star was estimated by Chevalier et al. (1999) to be a K7V star. With an 18.95 hr period, $1.4 M_{\odot}$ neutron star, and mass ratio $q = 0.33$ (Welsh, Robinson, & Young 2000) we expect $\log g = 3.93$. Plausible uncertainties in q have a very small effect on this.

Like MM Vel, Aql X-1 is very crowded in ground-based observations making optical photometry rare and somewhat uncertain. The primary source is Chevalier et al. (1999).

5. Spectral Energy Distributions

5.1. Fitting Methodology

We begin by fixing the spectral type and reddening to the values estimated in Section 4. We then adopt a suitable spectrum from Hauschildt, Allard, & Baron (1999) for the companion star, redden it using the extinction law of Fitzpatrick (1999), and evaluate synthetic photometry of the reddened companion in the bandpasses of interest using the SYNPHOT synthetic photometry package (Laidler et al. 2005). One of the primary advan-

tages of this approach is to correctly allow for red leak from the companion star’s red light into the UV bandpasses. In a similar way, we calculate models for the accretion light over the range of parameters of interest, redden them, and perform synthetic photometry. This gives us tabulated fluxes for the two components, allowing us to fit the composite model to the UV photometric data in its native form with the normalization of each component as a free parameter.

We adopt black body models for the disk emission. A single-temperature model provides the simplest characterization of the data. For comparison with the results of McClintock et al. (2003) on XTE J1118+480, we also fit models where the UV emission comes from the inner edge of a multi-color black body disk. Note that this model explicitly assumes that the accretion rate is independent of radius (steady-state), so this may not be an accurate description of the behavior of a quiescent disk. In the case of GU Mus, we also compare a model of a slab of recombining hydrogen implemented in SYNSPEC, described by an effective temperature, a column density, and an area. It can be seen from Figs. 2–5 that although we have considered the contribution of the companion star, both directly and via its red-leak, in every case the companion contributions in the UV are much smaller than those from the accretion disk and so have very small impact on our fitting results.

5.2. GU Mus = X-ray Nova Muscae 1991

Since the spectral type of the secondary star in GU Mus is relatively well constrained we fix its spectral type. Published optical photometry spans rather a large range, but this is consistent with observed short term variability (Hynes et al. 2003). We fix the brightness of the companion star spectrum to lie at the lower envelope of the optical points. The brightness adopted is not critical, as this results in only a 5% contribution to the F330W filter, and negligible impact in other UV passbands.

The residual photometric SED visually appears well described by a single-temperature blackbody with temperature $T = 13000 \pm 1400$ K and area about 0.3% of the projected area of a tidally truncated accretion disk ($\sim 0.9R_{\text{Roche}}$; Whitehurst & King 1991) at 5.89 kpc. This fit is shown in Fig. 2. Formally the fit yields $\chi^2 = 8.25$

with one degree of freedom, so the fit is not as good as might be expected. The inferred blackbody is small compared to the accretion disk, and a region of radius 6% of the maximal accretion disk radius could readily account for this. It could be interpreted as either the accretion stream-impact point, or a hot inner annulus of the disk. The effect of uncertainty in the companion star is indeed small. Reducing its contribution to zero, or doubling it, changes the derived temperature by less than 1000 K.

For comparison to XTE J1118+480, we also performed an analogous fit with a multi-color black body disk. The best fit was obtained with $T_{\text{in}} = 21500 \pm 5700$ K, with the observed flux corresponding to $R_{\text{in}} \simeq 3 \times 10^9$ cm. This is hotter than found by McClintock et al. (2003), but the inner disk radius is actually inferred to be about the same.

Since the inferred area is so low, we can also consider the possibility that the light comes from a larger but optically thinner region of the disk. We should be cautious as we have introduced an additional free parameter and are now fitting three photometric bands with a three-parameter model. With this caveat, we find a statistically better fit with the optically thin model than with the black body, $\chi^2 = 3.34$ with no degrees of freedom. The best fit is found for a column density of $\sim 10^{20}$ cm $^{-2}$ and temperature $T = 16,100 \pm 2000$ K. Because the temperature is higher, while the optical depth remains relatively high, the required surface area is actually a little smaller than for the blackbody fit, corresponding to a region of radius about 4% of the maximal disk radius. Thus whether the UV is modeled by an optically thick or thin component, we come to the same conclusion: the emission originates from a hot region with a rather small projected cross-sectional area compared to that of the disk.

A potential advantage of the optically thin model can be seen in Fig. 2. The blackbody model predicts a substantial disk contribution in B , much higher than observed by several groups. The optically thin model predicts a much lower B flux than the blackbody model, so is much easier to reconcile with the archival optical photometry. Since the optical photometry were not simultaneous with the UV data, however, an alternative explanation is that the UV observations occurred when the ac-

cretion light was brighter than seen in the optical photometry. This is a quite plausible explanation, since the source is known to exhibit large amplitude optical flaring (Hynes et al. 2003). As discussed in Section 6.1 and shown in Fig. 7, GU Mus also has the highest inferred UV luminosity of the sample here, consistent with this being an unusually high state.

An additional argument against attributing the UV emission of quiescent BHXRTs to optically thin emission (in general, rather than in the specific case of GU Mus) is that this model predicts a large Balmer jump in emission. While our photometric observations cannot discriminate this, spectroscopic observations of other sources have been performed and reveal no such Balmer continuum emission. In both A 0620–00 (McClintock et al. 1995) and XTE J1118+480 (McClintock et al. 2003) simultaneous data either through or on either side of the Balmer jump shows no significant discontinuity, supporting an optically thick interpretation at least in these cases. In view of this evidence, we believe that the optically thick (black body) model is the most credible and apply this to the remaining sources. It is certainly possible, of course, that the optical depth varies from source to source, but without strictly simultaneous coverage across the Balmer jump we cannot constrain this.

5.3. V518 Per = GRO J0422+32

We consider both M1V and M5V spectral types for V518 Per (Fig. 3). Allowing that the strength (and possibly temperature) of the hot component could vary, both possibilities are acceptable, although M5V appears to provide a better fit in the optical region of the SED. Both models suggest a large or dominant accretion contribution in the optical, and a measurable one in the infrared, in agreement with observations.

Both spectral types produce negligible UV light (even allowing for red leaks) and consequently, the hot component derived is largely independent of the assumed companion spectral type. For an M1 companion we find $T = 5200 \pm 2200$ K, whereas for M5 we find $T = 5100 \pm 2000$ K. In both cases, the hot component has an area 0.3% of the projected area of a tidally truncated disk at 2.49 kpc (as was also found in GU Mus). If we instead use a multi-color black body disk model, we ob-

tain a similar temperature, $T_{\text{in}} = 5800 \pm 2900$ K, with a rather larger inner radius than GU Mus, $R_{\text{in}} \simeq 13 \times 10^9$ cm.

5.4. MM Vel = X-ray Nova Velorum 1993

While a UV excess is strongly detected in MM Vel, we encountered difficulties in properly fitting it. Neither the black body nor optically thin recombination model could reproduce the combination of a rising spectrum from F330W to F250W and the non-detection in F220W. We show in Fig. 4 a representative 12,000 K model but do not feel it appropriate to quote a formal fit in this case. This model over-predicts the F220W flux, but since the discrepancy is less than 3σ this may be a statistical fluctuation. We note that the source size implied by a 12 000 K black body model is smaller than in the other systems in this paper, just 0.06% of the estimated projected area of a tidally truncated disk, which may be another indication that there are differences in the source of the UV emission in this system. Using a multi-color black body disk model we derive rather an inner temperature of $T = 17800$ K, with a lower limit ($1 - \sigma$) of 9100 K, and the upper limit unconstrained. For the best fit, the inner disk radius derived is $R_{\text{in}} \simeq 1.1 \times 10^9$ cm.

It is possible that the F250W flux is high due to the contribution from the Mg II line which is known to be strong in quiescent LMXBs (McClintock et al. 1995; McClintock & Remillard 2000; McClintock et al. 2003). Another explanation for the discrepancy is intrinsic source variability. To test this, we examined individual F330W observations (which by design bracketed the F250W and F220W observations). We found the F330W flux showed a standard deviation of only 15% of the mean with no systematic trend, small enough to be a constant flux within uncertainties. This does not rule out variability as an explanation, either for a low F220W flux or a high F250W one, but provides no evidence for such an explanation.

5.5. Aql X-1

Aql X-1 has the least well-constrained optical SED of the sources considered, but as in the other cases, this has relatively little impact on the interpretation of the UV data as all plausible compan-

ion star spectra make negligible UV contribution. We can obtain a good fit to the UV data with a black body of $T = 9300 \pm 700$ K and about 7.5% of the area of a tidally truncated disk. The available data and model fit are shown in Fig. 5. With the alternative multi-color black body fit, we obtain $T_{\text{in}} = 12400 \pm 1500$ K and $R_{\text{in}} \simeq 7 \times 10^9$ cm.

6. Discussion

6.1. Comparison between UV and X-ray luminosities

We compile the SEDs in νF_ν form in Fig. 6. McClintock et al. (2003) suggested that the shape of the UV spectrum could discriminate between black hole and neutron star systems. That does not seem to be borne out by our larger sample where it instead appears that the shape of the UV spectrum reflects random variance in the location of the peak of the spectrum from system to system. Note in particular that both GU Mus and Aql X-1 can be well fitted by black body models, but that it is the black hole system, not the neutron star, which has the higher temperature of the pair. As can be seen from Fig. 6, however, our sample does seem to bear out the trend that the X-ray to UV ratio is higher in NSXRTs than in their black hole counterparts. Both Cen X-4 (McClintock & Remillard 2000) and Aql X-1 show SEDs rising from UV to X-ray, whereas the black hole systems all decline. This result in itself is not new, and bears out the earlier realization that black holes have optical/UV non-stellar luminosities exceeding their X-ray luminosities, whereas in neutron stars this is reversed (Campana & Stella 2000; see also Narayan & McClintock 2008). The advantage we have, however, is that by working with the almost pure UV accretion light, we are not at the mercy of uncertainties in the stellar contribution; we can directly compare UV accretion light with X-ray emission.

We can perform the comparison more rigorously by examining the relationship between X-ray and (dereddened) UV luminosities. In Fig. 7 we compile these data for the four sources in our sample, and for archival STIS spectra of A 0620–00, Cen X-4, and XTE J1118+480 (McClintock & Remillard 2000; McClintock et al. 2003), and ACS photometry of V404 Cyg (Hynes et al. 2009). X-ray data are taken from Garcia et al.

(2001) for A 0620–00 and V518 Per, from Campana et al. (2004) for Cen X-4, from Narayan, Garcia, & McClintock (1997) for Aql X-1, from Sutaria et al. (2002) for GU Mus, from Hameury et al. (2003) for MM Vel, from McClintock et al. (2003) for XTE J1118+480 and from Hynes et al. (2009) for V404 Cyg. It should be noted that only XTE J1118+480, and V404 Cyg have *simultaneous* UV and X-ray measurements. As anticipated, the neutron star systems appear systematically above those containing black holes (ranks 1 and 2 out of 8 ranked by L_X/L_{UV}). All neutron stars have $L_X > L_{\text{UV}}$ and all black holes have $L_X < L_{\text{UV}}$. Note in particular that GU Mus is securely detected at a much higher UV luminosity than either of the NS systems, even though it is much fainter at X-ray energies.

This suggests that black hole systems are less efficient at producing X-rays from accreted material than neutron stars (assuming that the UV luminosity is a measure of the accretion rate feeding the compact objects). This is not a new idea, of course, and similar claims have been made based on a comparison of X-ray luminosities alone or in combination with estimates of the non-stellar optical light (Narayan, Garcia, & McClintock 1997; Campana & Stella 2000; Garcia et al. 2001; Hameury et al. 2003; Narayan & McClintock 2008). However, comparison of the UV flux with the X-ray flux gives us more confidence that differences reflect efficiency of production of X-rays, rather than differences in mass accretion rate. Furthermore, in the case of Aql X-1, the UV properties are very similar to those of the black hole sample, suggesting that the difference between the two is indeed driven by X-ray differences rather than UV ones.

6.2. The UV light source

Where we are able to obtain good fits to the SEDs, they are characterized by temperatures higher than expected in quiescent accretion disks, which should be $\lesssim 3000$ K (Menou 2002), and have much smaller emitting areas than the accretion disk. Previously published spectroscopic observations show similar trends. A 0620–00 was fitted by McClintock et al. (1995) with a 9,000 K black body with area 1/80th of that of the accretion disk. XTE J1118+480 was described by McClintock et al. (2003) as being fitted with a multicolor black body disk model with inner edge temperature 13,000 K. Cen X-

4 exhibits a UV spectrum that rises monotonically in νF_ν , indicating a hot source of emission (McClintock & Remillard 2000). The most likely nature of a localized, hot region of UV emission would seem to be the accretion stream impact point, but a hot inner edge to the accretion disk near a transition to an evaporated flow might be another possibility.

If the UV emission originates at the stream-impact point we would expect the UV luminosity to come from energy liberated in falling to the stream-impact point. For the luminosity of the hot source we integrate the unreddened black body fit to the UV photometry. We can estimate the maximum energy we might expect to release as half the binding energy of material at the circularization radius in the accretion disk. If the disk extends beyond the circularization radius, then the stream-impact point will be higher in the potential well and less energy will be liberated. For GU Mus, we require a very high accretion rate of about $4 \times 10^{-9} M_\odot \text{ yr}^{-1}$ to explain the UV luminosity if this is sustained. This can be compared to the estimated mass required to power the 1991 outburst of $10^{-8} M_\odot$. At this accretion rate, the mass required by the outburst could be supplied in ~ 3 years, whereas we have only seen one outburst of GU Mus, suggesting a recurrence time at least ten times larger than this. If the energy source of the UV emission is to be gravitational energy liberated at the hot-spot, we then require that the accretion rate, and UV luminosity, be highly variable and that the GU Mus observations were well above the average level as suggested earlier.

Performing similar calculations for the other sources yields mass transfer rates from the donor star of $3 \times 10^{-10} M_\odot \text{ yr}^{-1}$ for V518 Per, $1 \times 10^{-10} M_\odot \text{ yr}^{-1}$ for MM Vel, and $3 \times 10^{-9} M_\odot \text{ yr}^{-1}$ for Aql X-1. The values for V518 Per and MM Vel are substantially below that of GU Mus, and do not impose strong constraints, but that for Aql X-1 is comparably high. In this case, we have observed multiple outbursts, and so have a much more secure estimate of the time-average accretion rate. Rutledge et al. (2001) have estimated this at $2.5 \times 10^{-10} M_\odot \text{ yr}^{-1}$ (assuming a 5 kpc distance as we have used). This again is a discrepancy of an order of magnitude with the observed UV brightness.

Both GU Mus and Aql X-1 would require mass

transfer rates from their donor stars in excess of $10\times$ the plausible average rate to explain the UV light source as a stream-impact point at or outside the circularization radius in the disk, and so this explanation seems untenable. An alternative explanation is that the UV originates much deeper in the gravitational potential well, in the inner disk just outside the transition radius, as suggested by Campana & Stella (2000) and specifically considered for XTE J1118+480 by McClintock et al. (2003). Fitting our photometry with multi-color black body disk models yields comparable results to XTE J1118+480, with high temperatures and radii of order $1\text{--}10 \times 10^9 \text{ cm}$, comparable to expected transition radii of $1000\text{--}10,000 R_{\text{sch}}$. In this case a lower mass accretion rate is needed to supply the energy than if the UV emission originates at the stream-impact point. If some of the accretion stream overflows the disk, it will impact closer to the compact object and could provide an alternative mechanism for increased heating of the inner disk although in this case we might expect to see evidence for stream-overflow in phase-resolved spectroscopy of quiescent LMXBs. We note that another explanation, that the inner disk is simply heated by the X-ray source, cannot adequately explain the UV emission when we see UV luminosities comparable to or exceeding the X-ray luminosity.

7. Conclusions

We have found UV excesses in four quiescent LMXB systems, three black hole systems and one containing a neutron star. In every case, the UV detection is secure and greatly exceeds that expected by the companion star. The spectral shapes are heterogeneous, and black body models require a variety of temperatures and emitting areas. In some cases a good fit could alternatively be obtained with an optically thin recombination spectrum, although this would be inconsistent with the limited spectroscopic observations of other sources across the Balmer jump suggesting it is not present in emission in those cases. In general, the temperatures are higher (sometimes much higher) than expected for quiescent disks, and the UV light sources are also much smaller than the whole disk. The most likely origin of the stream-impact point can probably be discounted as the requisite accretion rates for both GU Mus

and Aql X-1 are at least an order of magnitude above estimates, or limits on, the time-averaged accretion rate. It is therefore more likely that the UV emission originates from a hot inner region of the disc.

This work includes observations with the NASA/ESA *Hubble Space Telescope*, obtained at STScI, which is operated by AURA Inc. under NASA contract No. NAS5-26555. Support for *HST* proposal GO 10253 was provided by NASA through a grant from STScI. R.I.H. also acknowledges support by the National Science Foundation under Grant No. AST-0908789. This work has made use of the NASA Astrophysics Data System Abstract Service.

Facilities: HST (ACS).

REFERENCES

- Beekman G., Shahbaz T., Naylor T., Charles P. A., Wagner R. M., Martini P., 1997, *MNRAS*, 290, 303
- Callanan P. J., Garcia M. R., McClintock J. E., Zhao P., Remillard R. A., Haberl F., 1996, *ApJ*, 461, 351
- Campana, S., & Stella, L. 2000, *ApJ*, 541, 849
- Campana S., Israel G. L., Stella L., Gastaldello F., Mereghetti S., 2004, *ApJ*, 601, 474
- Casares J., Martin A. C., Charles P. A., Martin E. L., Rebolo R., Harlaftis E. T., Castro-Tirado A. J., 1995, *MNRAS*, 276, L35
- Casares J., Martin E. L., Charles P. A., Molaro P., Rebolo R., 1997, *New A*, 1, 299
- Chevalier C., Ilovaisky S. A., 1996, *A&A*, 312, 105
- Chevalier C., Ilovaisky S. A., Leisy P., Patat F., 1999, *A&A*, 347, L51
- Cox A. N. (Ed.), 2000, *Allen's Astrophysical Quantities*, 4th Edn., Springer
- della Valle M., Benetti S., Cappellaro E., Wheeler C., 1997, *A&A*, 318, 179
- della Valle M., Masetti N., Bianchini A., 1998, *A&A*, 329, 606
- Fender R. P., Gallo E., Jonker P. G., 2003, *MNRAS*, 343, L99
- Filippenko A. V., Leonard D. C., Matheson T., Li W., Moran E. C., Riess A. G., 1999, *PASP*, 111, 969
- Fitzpatrick E. L., 1999, *PASP*, 111, 63
- Froning, C. S., Cantrell, A. G., Maccarone, T. J., et al. 2011, *ApJ*, 743, 26
- Garcia M. R., Callanan P. J., McClintock J. E., Zhao P., 1996, *ApJ*, 460, 932
- Garcia M. R., McClintock J. E., Narayan R., Callanan P., Barret D., Murray S. S., 2001, *ApJ*, 553, L47
- Gelino D. M., 2004, *Rev. Mexicana Astron. Astrofis.*, 20, 214
- Gelino D. M., Harrison T. E., McNamara B. J., 2001, *AJ*, 122, 971
- Gelino D. M., Harrison T. E., 2003, *ApJ*, 599, 1254
- Gonzaga, S., et al. 2005, *ACS Instrument Handbook*, Version 6.0, (Baltimore: STScI)
- Gray R. O., Corbally C. J., 1994, *AJ*, 107, 742
- Hameury J.-M., Barret D., Lasota J.-P., McClintock J. E., Menou K., Motch C., Olive J.-F., Webb N., 2003, *A&A*, 399, 631
- Harlaftis E., Collier S., Horne K., Filippenko A. V., 1999, *A&A*, 341, 491
- Hauschildt P. H., Allard F., Baron E., 1999, *ApJ*, 512, 377
- Hynes R. I., 2005, *ApJ*, 623, 1026
- Hynes R. I., Charles P. A., Casares J., Haswell C. A., Zurita C., Shahbaz T., 2003, *MNRAS*, 340, 447
- Hynes, R. I., Bradley, C. K., Rupen, M., Gallo, E., Fender, R. P., Casares, J., Zurita, C., 2009, *MNRAS*, 399, 2239
- Jonker P. G., Steeghs D., Chakrabarty D., Juett A. M., 2007, *ApJ*, 665, L147
- King N. L., Harrison T. E., McNamara B. J., 1996, *AJ*, 111, 1675

- Koekemoer, A. M., Fruchter, A. S., Hook, R. N., & Hack, W. 2002, in Proc. The 2002 HST Calibration Workshop: Hubble after the Installation of the ACS and the NICMOS Cooling System, Eds. S. Arribas, A. Koekemoer & B. Whitmore, 337, Baltimore: STScI
- Laidler, V., et al., 2005, Synphot User's Guide, Version 5.0, Baltimore: STScI
- McClintock J. E., Horne K., Remillard R. A., 1995, ApJ, 442, 358
- McClintock J. E., Remillard R. A., 2000, ApJ, 531, 956
- McClintock J. E., Narayan R., Garcia M. R., Orosz J. A., Remillard R. A., Murray S. S., 2003, ApJ, 593, 435
- Menou K., Esin A. A., Narayan R., Garcia M. R., Lasota J.-P., McClintock J. E., 1999, ApJ, 520, 276
- Menou, K. 2002, ASP Conf. Ser. 261: The Physics of Cataclysmic Variables and Related Objects, 387
- Narayan R., Garcia M. R., McClintock J. E., 1997, ApJ, 478, L79
- Narayan, R., & McClintock, J. E. 2008, New A Rev., 51, 733
- Orosz J. A., Bailyn C. D., McClintock J. E., Remillard R. A., 1996, ApJ, 468, 380
- Pavlovsky, C., Koekemoer, A. & Mack, J., Eds., HST Data Handbook for ACS v4.0, Baltimore: STScI
- Remillard R. A., McClintock J. E., Bailyn C. D., 1992, ApJ, 399, L145
- Reynolds M. T., Callanan P. J., Filippenko A. V., 2007, MNRAS, 374, 657
- Riess, A., Mack, J., Time Dependence of ACS WFC CTE Corrections for Photometry and Future Predictions, Instrument Science Report ACS 2004-006, Baltimore: STScI
- Rutledge R. E., Bildsten L., Brown E. F., Pavlov G. G., Zavlin V. E., 2001, ApJ, 559, 1054
- Shahbaz T., van der Hooft F., Charles P. A., Casares J., van Paradijs J., 1996, MNRAS, 282, L47
- Sirianni, M., et al. 2005, PASP, 117, 1049
- Sutaria F. K., et al., 2002, A&A, 391, 993
- Webb N. A., Naylor T., Ioannou Z., Charles P. A., Shahbaz T., 2000, MNRAS, 317, 528
- Welsh W. F., Robinson E. L., Young P., 2000, AJ, 120, 943
- Whitehurst R., King A., 1991, MNRAS, 249, 25
- Zhao P., Callanan P., Garcia M., McClintock J., 1994, IAU Circ., 6072

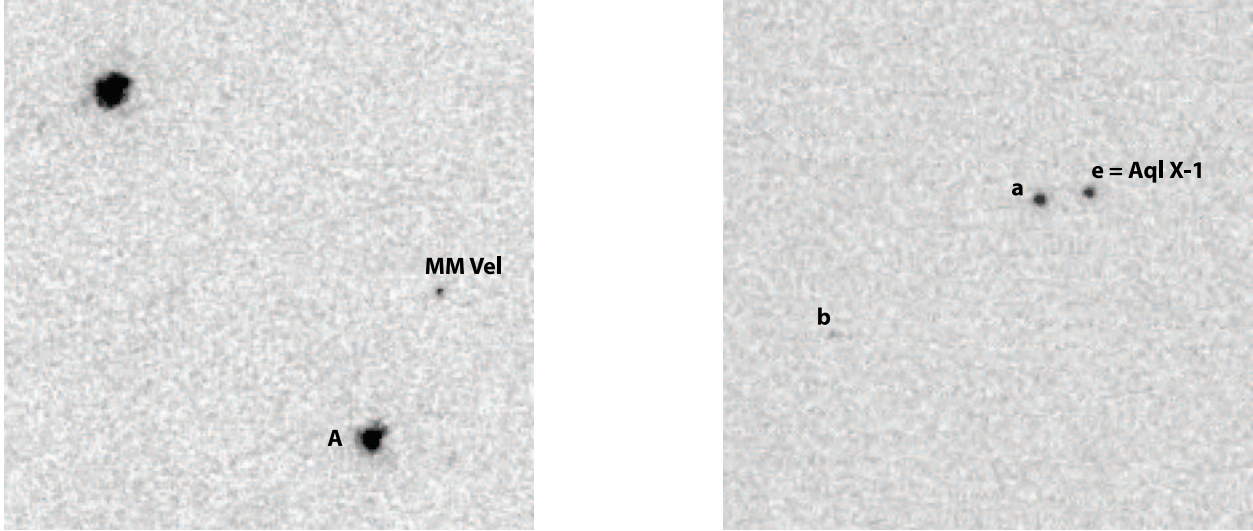


Fig. 1.— F330W images of the field of MM Vel (left) and Aql X-1 (right). The fields are 5" square, and labels are from Filippenko et al. (1999) and Chevalier et al. (1999). The orientation is conventional (north at top and east to the left). This means that the image of Aql X-1 is inverted with respect to that of Chevalier et al. (1999).

Table 1: Log of ACS/HRC observations.

Object	Date	Filter	UT range	Total time (s)	Count rate (s ⁻¹)	F_λ (10 ⁻¹⁸ erg cm ⁻² s ⁻¹ Å ⁻¹)
GU Mus	2004 Oct 12	F330W	07:19–09:35	1920	6.63 ± 0.10	14.84 ± 0.22
		F250W	07:30–09:11	1860	2.73 ± 0.07	13.07 ± 0.32
		F220W	07:47–09:25	1280	0.75 ± 0.08	6.11 ± 0.63
V518 Per	2005 Oct 31	F330W	12:34–16:30	2880	0.62 ± 0.06	1.39 ± 0.12
		F250W	12:44–16:08	2440	0.10 ± 0.04	0.48 ± 0.21
		F220W	12:59–16:20	1480	-0.06 ± 0.07	-0.53 ± 0.57
MM Vel	2004 Dec 11	F330W	10:45–13:05	1720	0.99 ± 0.08	2.20 ± 0.17
		F250W	10:54–12:42	1780	0.51 ± 0.05	2.43 ± 0.25
		F220W	11:12–12:54	1200	-0.01 ± 0.07	-0.10 ± 0.58
Aql X-1	2004 Sep 22	F330W	20:10–00:04	2880	2.18 ± 0.06	4.87 ± 0.14
		F250W	20:20–23:43	2360	0.56 ± 0.05	2.68 ± 0.25
		F220W	20:34–23:54	1540	0.06 ± 0.07	0.49 ± 0.60

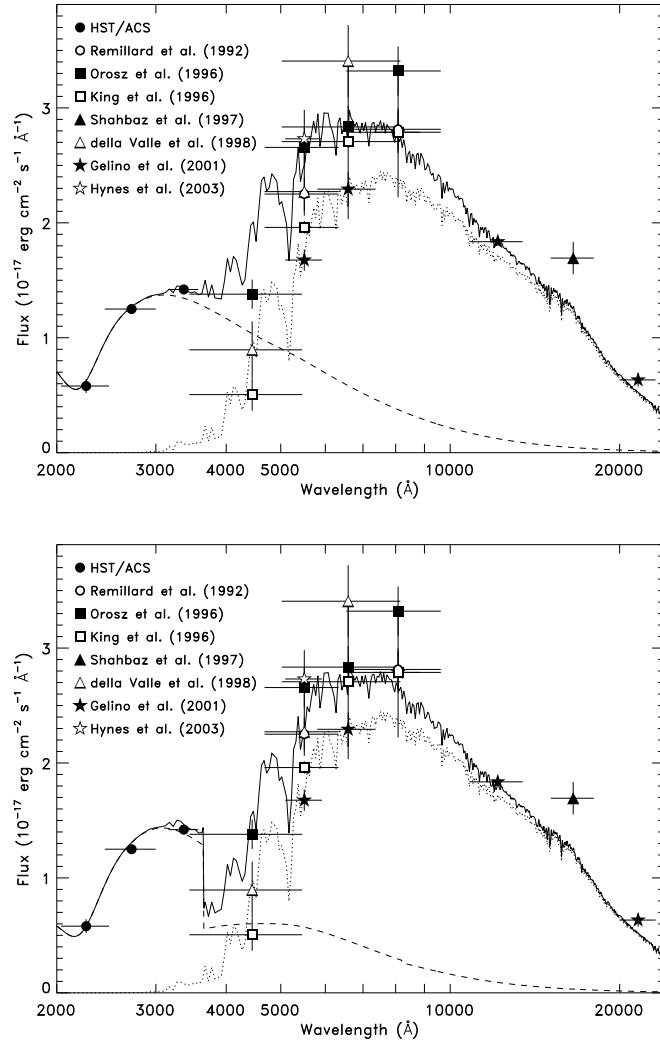


Fig. 2.— Black body plus stellar fit to data on GU Mus (upper panel) and optically thin recombination spectrum plus stellar fit (lower panel). Wavelength uncertainties shown on the photometric points represent the FWHM of the filter bandpasses. In this and subsequent plots, the dotted line represents the stellar component, the dashed line is the accretion component, and the solid line is the sum of the two.

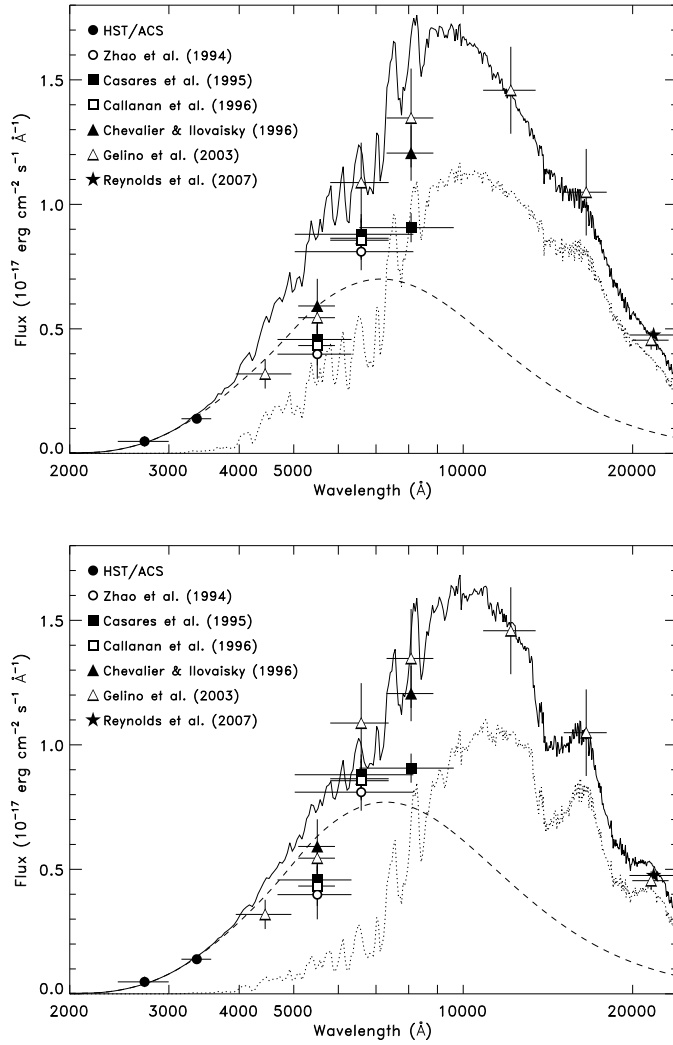


Fig. 3.— Black body plus stellar fit to data on V518 Per. The upper panel is for an M1V companion, the lower panel for M5V.

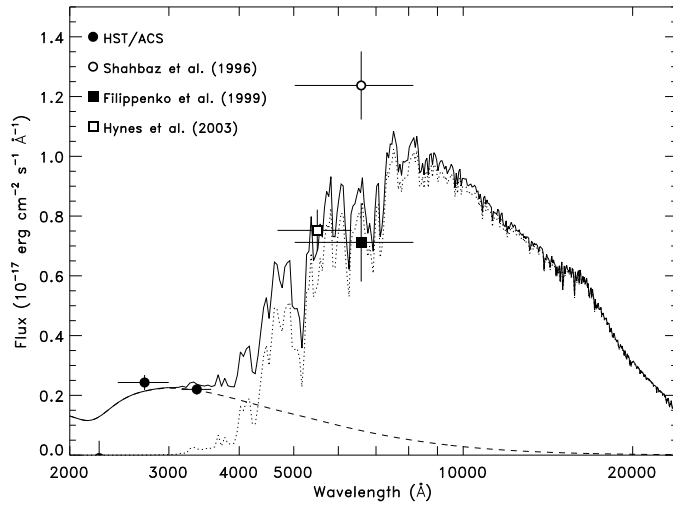


Fig. 4.— Black body plus stellar fit to data on MM Vel

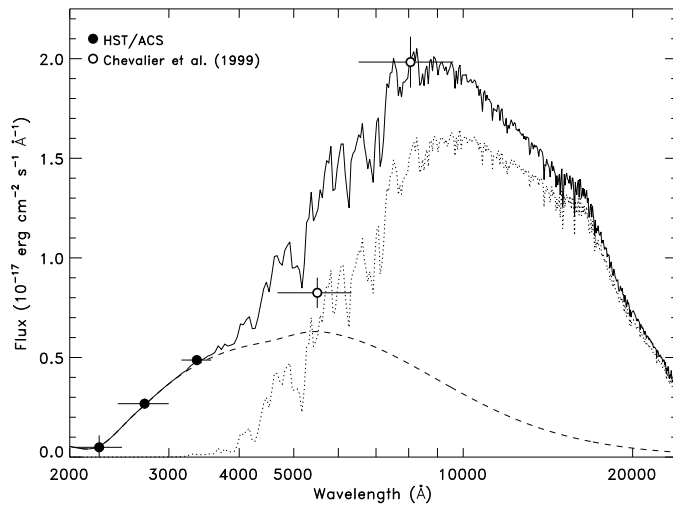


Fig. 5.— Black body plus stellar fit to data on Aql X-1

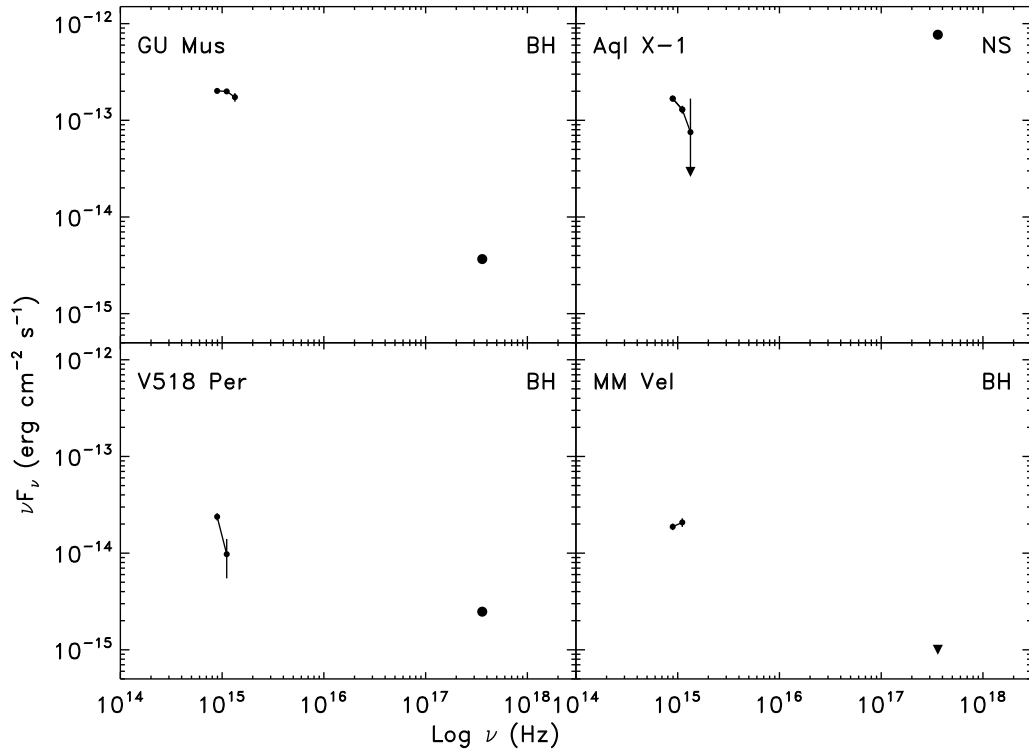


Fig. 6.— UV–X-ray spectral energy distributions of the four targets observed here. We do not show the F220W non-detections of V518 Per and MM Vel. We also include X-ray measurements taken from Sutaria et al. (2002) for GU Mus, Garcia et al. (2001) for V518 Per, Hameury et al. (2003) for MM Vel, and Narayan, Garcia, & McClintock (1997) for Aql X-1. The black holes all decline in νF_ν from UV to X-rays, the one neutron star increases.

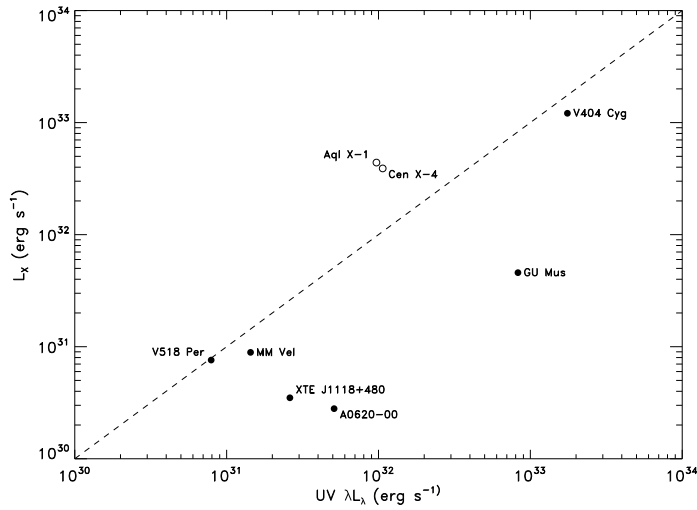


Fig. 7.— The relationship between UV and X-ray luminosities of six quiescent BHXRTs (filled circles) and two NSXRTs (open circles). The dashed line corresponds to $\lambda L_\lambda = L_X$. Lines parallel to this are loci of constant L_X/L_{UV} . Uncertainties in distance will also move a source parallel to this line. Uncertainties in dust extinction will move a source horizontally in the diagram.